Publ. Astron. Obs. Belgrade No. 107 (2025), 91 - 94 *Poster*
http://doi.org/10.69646/14sbac14p

PHOTOMETRIC PERIODS OF M31 LBV AF AND IDENTIFIED VIA STRUCTURE EMINENCE FUNCTION METHOD

TS. GEORGIEV[1], A. VALCHEVA[2] and P. NEDIALKOV[2]

[1]*Institute of Astronomy and National Astronomical Observatory, Bulgarian Academy of Sciences, 72 Tsarigradsko Chaussee Blvd., 1784 Sofia, Bulgaria*
E–mail: tsgeorg@astro.bas.bg

[2]*Department of Astronomy, Faculty of Physics, Sofia University, 5 James Bourchier Blvd., 1164 Sofia, Bulgaria*

Abstract. We use B-band historical light curve of AF And in the time interval 1918-1990 to search for photometric periods applying Structure eminence function (SEF) method and its derivative the Periodograph function (PGF). Periods of 3.90 ± 0.10 yr and 4.55 ± 0.10 yr are found. SEF is the dependence of the structure amplitude on the structure time length and extracts and uses profiles of these structures. The positions of the SEF maxima mark eminent periods and quasi periods.

1. INTRODUCTION

Various methods exist for deriving periods in time series or light curves (LCs). The periodogram methods CLEAN (Roberts, 1987) and Lomb-Scargle (Lomb, 1976; Scargle, 1982), hereafter C&LS, are widely used in Astronomy.

Our Structure Eminence Function (SEF) method identifies and characterizes repetitive structures (patterns) responsible for the periodicity. SEF represents the average amplitude of the structure as a function of the time length of the structure ($E(t)$, Eq.1, Figs.(c)). The peak positions in the SEF mark significant periods and quasi-periods. After SEF, we use Periodograph Function (PGF), which enhances the visibility of the SEF peaks ($G(t)$, Eq.2, Figs.(d)).

The SEF method poses higher time resolution than the C&LS methods, with an improvement of up to 2 times. This advantage likely arises from its ability to operates with concrete profiles (shapes) of structures. Additionally, the structure profile may provide useful insights on the nature of the periodicity. Four variations of the SEF method can be distinguished according to the used preparatory procedures: resampling with a constant time step versus no resampling, as well as with local or global detrending. The SEF method was tested on various time series and its results were compared with the results of other periodogram analyses (Georgiev 2023, hereafter G23). Clearly prominent photometric period of 5.7 yr was found in the LCs of the LBV η Carinae (Georgiev et al. 2024, hereafter G+24).

In this study, an interpolated resampling with a step of 0.05 yr is performed for deriving a suitable input LCs (Figs.(a)). The resampling omits many sharp local LC peaks, but it (i) ensures uniform use of all parts of the LC and (ii) traces better the SEF humps. Detrending - the removal of large scale trend from the input LC - is

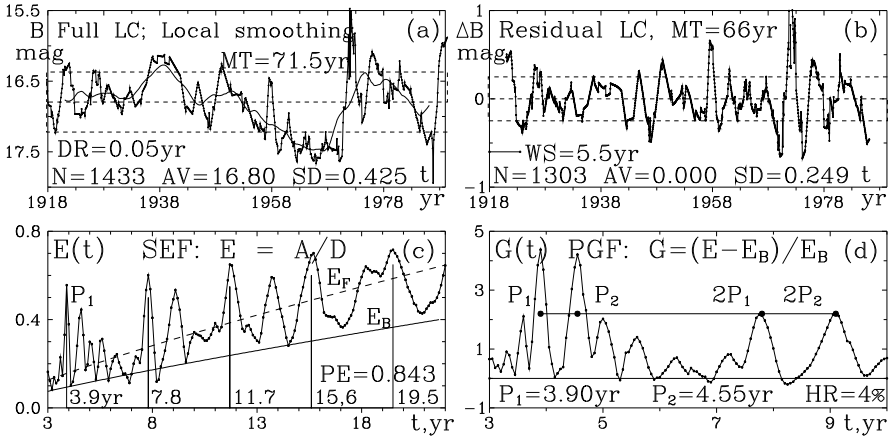

Figure 1: SEF (c) and PGF (d) build after resampling and local detrending of the 'Full LC' of AF And. See the text.

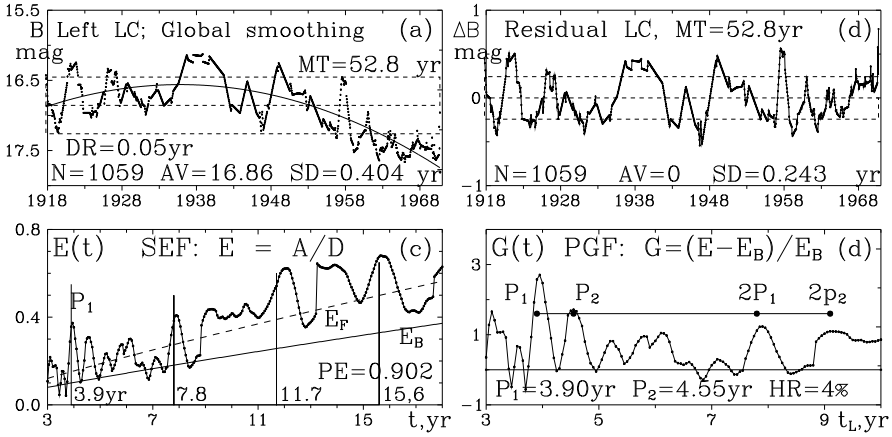

Figure 2: SEF (c) and PGF (d) build after resampling and global detrending of the 'Left part' of the LC of AF And. See the text.

obligatory when SEF method is applied. For this purpose, a smoothed version of the input LC is extracted, resulting in the residual LC (RLC).

The RLC (Figs. (b)) is a flat version of the input LC which is used for the SEF building. The RLC is also suitable as input for C&LS methods (G+24). Local smoothing through moving average is performed and shown in Fig.1a. The window size (WS) is 5.5 yr or 110 resampled data points (dp). This WS ensures the optimal prominence of the SEF/PGF maxima at about 4 yr. Global smoothing is performed through a second-degree polynomial fit of the input light curve, as shown in Fig. 2a.

2. AMPLITUDE AND NOISE OF THE STRUCTURE. SEF AND PGF

Let's consider RLC (t_i, z_i), $i = 1...N$ dp with constant data step δt, zero average value (AV) and relevant standard deviation (SD). Suppose this RLC contains significant

repetitive structure with a size of l dp or a time length $T_L = L \times \delta t$. Our code identifies the length L of the basic period after checking numerous LC segments with lengths $L = L_1...L_2$ as follows.

For every L, we pull up the first L RLC values, $z_i, i = 1...L$, and put them into an initially empty set with cell numbers $j = 1...L$. Then, we add there the next L dp, $z_i, i = L + 1...L + L$, from the RLC. Later, we add the next L dp, etc. The (integer) number of possible adds is $K = N/L$. In the end, every j-th cell, containing K adds, has relevant AV a_j and SD d_j. So, the structure with length L dp is described by a signal profile a_j and a noise profile d_j. Finally, we derive the average amplitude $A_L =< |a_j| >_L$ and average noise $D_L =< d_j >_L$. Note that A_L gathers absolute values $|a_j|$, i.e. A_L is one-side average amplitude of the structure. Applying SEF method, we extract numerous RLS segments with lengths $L = L_1...L_2$, characterizing each of them by A_L and D_L. In this study, we specify $L_1 = 20$ dp. For at least $K = 3$ additions (for statistically significant AV and SD), the code derives and uses $L_2 = N/3$.

Every significant repetitive structure of the RLC produces local maximum in the amplitude function A and local minimum of the noise function D. Therefore, we have to define the dimensionless SEF (Figs.(c)) as follows:

$$E_L = A_L/D_L; \qquad E(t) = A(t)/D(t). \tag{1}$$

The position of the leftmost local SEF maximum marks the basic period P. The periods $2P$, $3P$, etc. cause additional default maxima.

The SEF fits, E_F, shown in Figs.(c) (dashed curves), are power functions. In log-log scale, they are straight lines. The SEF maxima become more prominent when the SEF background is removed. Therefore, the background line, which bounds 90% of the SEF points from below, is derived by shifting the SEF line downward. After transforming it back into linear scale, the SEF background line becomes a power function E_B with a power exponent (PE) similar to that of the E_F (Figs. (c), solid curves). As a result, we define the dimensionless PGF using the SEF values E and the corresponding SEF background values E_B (see Figs.(d)), as follows:

$$G_L = (EE_B)/E_B; \qquad G(t) = (E(t)E(t)_B)/E(t)_B. \tag{2}$$

In the PGF, the SEF maxima are more prominent and the time resolution of the SEF method can be estimated better (Figs.(d)).

3. DERIVING PHOTOMETRIC PERIODS OF AF AND

We analyzed the historical B-band LC of the M31 LBV AF And in the time interval 1918-1990, compiled by Gantchev et al. (2017). The original 'Full LC' (Fig.1a) contains 393 dp in the monitoring time (MT) of 71.5 yr. The section of this LC prior to the eruptions in 1971-1973, referred to as the 'Left LC' (Fig.2a), contains 280 dp in the MT of 52.8 yr (1918-1970).

After resampling with a step of 0.05 yr, the input LCs for the 'Full LC' and the 'Left LC' contain $N = 1433$ dp and $N = 1059$ dp, respectively. The 'Full LC' is detrended using a moving average applied to the resampled LC with a WS of 5.5 yr (110 dp). The 'Left LC' is detrended by fitting a 2nd-degree polynomial to the resampled LC (Figs.(a),(b)).

Figures (a) show the input (resampled) LCs and their smoothed versions. Figures (b) show the corresponding RLCs (the differences between the smoothed and input LC). Horizontal lines show AV level and AV±SD levels. In Fig. 1b, due to the local smoothing, the RLC edges with lengths $5.5/2 = 2.25$ yr (55 dp) each, are lost. Note that we use RLC in magnitude differences $\Delta B = (B_{smooth} B_{resampled}$ and the positive values ΔB correspond to increased brightness.

Figures (c) show the SEFs (Eq. 1) derived from the RLCs shown in Figs.(b). For $K = 3$ segment additions, the maximal checked segment lengths are $66/3 = 22$ yr or $52.8/3 = 17.7$ yr), respectively. Here, E_F and E_B are the fits of the SEF and SEF background, as power functions. Further, E_B is used for deriving of PGF (see Figs. (d) and Sect. 2). PE is the power exponent. The leftmost SEF maximum marks the basic period, $P_1 = 3.90$ yr. Its default larger counterparts, $2P_1, 3P_1$, etc, cause other maxima. Shorter counterparts, e.g. $P_1/2$ (see G23), are not detected here. However, a second period, $P_2 = 4.5$ yr, is also clearly observable.

Figures (d) show the initial parts of the PGFs (Eq. 2). The peaks of the periods P_1 and P_2, as well as $2P_1$ and $2P_2$ are clearly pronounced. The relative hump resolution (HR) of the SEF method, the half width at the half of the maximum, at about $P = 4$ yr, is about 4% or 0.16 yr. However, the positions of the hump peaks may be located with an accuracy of at least ±0.1 yr. We assume 0.1 yr to be the SD of our period estimation.

4. SUMMARY

We analyzed the 20th century 'Full LC' and 'Left LC' of the historical LC of AF And, resampled with step of 0.05 yr. We apply universal local detrend of the 'Full LC' and a global detrend of the 'Left LC'. In both cases, we found two well prominent periods: $P_1 = 3.90 \pm 0.10$ yr and $P_2 = 4.55 \pm 0.10$ yr.

In addition, applying a local detrend of the 'Left LC' (not shown here), we found the same periods. Applying the same analysis after resampling with step of 0.1 yr (not shown here), we found periods of 3.9 yr and 4.6 yr.

We can speculate that one of these periods may corresponds to probable orbital period, similarly to the period of 4.7 yr in the case of η Carinae (see G+24) and the other one is of uncertain origin.

Acknowledgements

This study is financed by the European Union – NextGenerationEU, through the National Recovery and Resilience Plan of the Republic of Bulgaria, project SUMMIT BG-RRP-2.004-0008-C01. We also acknowledge partial support by Bulgarian National Roadmap for Research Infrastructure Project D01-326/04.12.2023 of the Ministry of Education and Science of the Republic of Bulgaria.

References

Gantchev, G., Nedialkov, P.: 2019, *IAU Symposium 339*, 87, doi: 10.1017/S1743921318002284
Georgiev, Ts.: 2023, *Bulg. Astron. J.* **38**, 120 [G23], bibcode 2023BlgAJ..38..120G
Georgiev, Ts., Valcheva, A., Nedialkov, P., Stefanov, S,, Moyseev, M.: 2024, *Bulg. Astron. J.*, submitted, [G+24]
Lomb, N. R.: 1976, *Astrophys.Sp.Sci*, **39**, 447, doi 10.1007/BF00648343
Roberts, D. H., Lehar J., Dreher J. W.: 1987, *Astron. J.*, **93**, 968, doi 10.1086/114383
Scargle J. D.: 1982, *Astrophys. J.*. **263**, 835, doi 10.1086/160554